Local and Global Dynamics of Transient Polymer Networks and Swollen Gels Anchored on Solid Surfaces

ARTICLE *in* THE JOURNAL OF PHYSICAL CHEMISTRY C · AUGUST 2007

Impact Factor: 4.77 · DOI: 10.1021/jp0728959

6 AUTHORS, INCLUDING:

Maria Gianneli
Attana AB
8 PUBLICATIONS **64** CITATIONS

SEE PROFILE

Local and Global Dynamics of Transient Polymer Networks and Swollen Gels Anchored on Solid Surfaces

M. Gianneli,[†,‡] P. W. Beines,[†] R. F. Roskamp,[†] K. Koynov,[†] G. Fytas,*[,†,‡] and W. Knoll[†]

Max Planck Institute for Polymer Research, Ackermannweg 10, 55128 Mainz, Germany, and Department of Materials Science and Technology, University of Crete and F.O.R.T.H., P.O. Box 1527, 71110 Heraklion, Greece

Received: April 13, 2007; In Final Form: July 4, 2007

We employ fluorescence correlation spectroscopy to study length dependent dynamics in transient and grafted cross-linked poly(*N*-isopropylacrylamide) (PNIPAAm) networks at different concentrations and cross-link densities, respectively. For nondilute PNIPAAm solutions, the molecular diffusants appear to sense local dynamics on the length scale of the mesh size obtained from photon correlation spectroscopy, whereas a polymer probe, comparable to the PNIPAAm size, reveals global chain motions. The relation of the tracer Brownian diffusion to the mesh size can be utilized to characterize permanently cross-linked and grafted PNIPAAm networks.

I. Introduction

Hydrogels are three-dimensional cross-linked polymer networks that incorporate a significant volume fraction of water. Since their water content and properties can be controlled by incorporating different amounts of hydrophilic and hydrophobic segments and cross linkers, hydrogels have attracted the attention of a wide variety of researchers working on biomedical applications. Tanaka and co-workers[1] first suggested the existence of hydrogels in the late 1970s while studying the water absorption properties of gels. Hydrogels containing interactive functional groups along the main polymeric chains are usually called "smart" or "stimuli-responsive" polymers. Such polymer gels can reversibly change their shape or other properties depending on external physicochemical factors such as temperature, pH, and ionic strength of the medium, solvent composition, electric or magnetic fields, light intensity,[2] and so forth. Poly(*N*-isopropylacrylamide) (PNIPAAm) has become perhaps the most popular member of this family, mostly because of its well-defined lower critical solution temperature (LCST) in water (around 32 °C), which is close to the body temperature. When this polymer is grafted to a solid surface,[3] the resulting coating shows temperature-dependent surface properties such as wettability.[4,5]

There has been great interest in studying particle transport and diffusion of solutes within macroporous, stiff-chained hydrogels, since this general problem[6] is important in a wide variety of biotechnological fields from cell encapsulation to controlled drug delivery. In all of these applications, the hydrogel act as a means of retarding the diffusion of the embedded molecules. While PNIPAAm-based gels have commonly been studied[7] as model systems for drug delivery applications, there are still many factors affecting the solute diffusion within these systems which are poorly understood. There is an extensive body of previous research on probe diffusion in nondilute polymer solutions,[9−11] but the area can hardly be considered mature because of the involved parameters as well as the presence of interactions. There is, however, a consensus about the role of the size of the diffusing species relative to the mesh size of the polymer network.

Here, we demonstrate how fluorescence correlation spectroscopy (FCS)[12] can quantitatively address the length scale dependent dynamics of supported PNIPAAm network films through the diffusion of tagged particles. The FCS technique is based on detecting the fluctuations of the fluorescent light intensity in a small observation volume, usually formed by the focus of a confocal microscope. While this method has been successfully utilized to study transport properties in various biological environments,[12] its applications in other soft systems are rare and only recently reported.[13] On the basis of the very small detection volume (approximately femtoliters) and its high sensitivity, FCS is perfectly suited to study the single tracer diffusion in thin, supported gels.

An additional motivation for the present work is to relate the diffusion retardation of a probe to the properties of the PNIPAAm network. We focus first on physical PNIPAAm networks in ethanol with controlled average mesh size as inferred by photon correlation spectroscopy (PCS). Using FCS and two different size tracer diffusants, we can probe both the local and the global transient polymer network dynamics. This tracer diffusion can then be utilized to provide structural information of grafted chemically cross-linked PNIPAAm films of different cross-linking density swollen also in ethanol. Moreover, the complementarity of the two related correlation techniques becomes apparent when employing them on the same system.

II. Experimental Section

Materials. *N*-Isopropylacrylamide (NIPAAm, Aldrich) was purified by recrystallization from a mixture of toluene/hexane (1:4) and dried in vacuum. Methacrylic acid (MAA, Aldrich) was distilled prior to use. 2,2′-Azobis(isobutyronitrile) (AIBN) was recrystallized from methanol. Dioxane used for the polymerization was distilled over calcium hydride. Tetramethylrhodamine cadaverine (Biotium) and all other reagents of

* Corresponding author.
† Max Planck Institute for Polymer Research.
‡ University of Crete.

10.1021/jp0728959 CCC: $37.00
Published on Web 08/11/2007

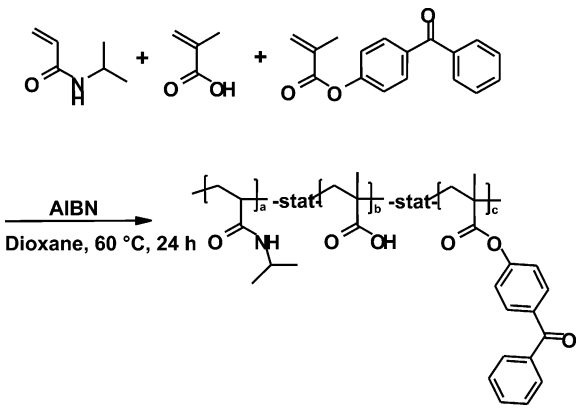

Figure 1. Polymerization reaction of the statistical PNIPAAm terpolymer.

analytical grade were used as received. The synthesis of 4-methacryloyloxybenzophenone (MaBP) monomer, 4-allyloxybenzophenone, 4-(3′-chlorodimethylsilyl)propyloxybenzophenone (silane**1**), and trifluoroacetyl *N*-succinimidylester is described elsewhere.[14]

Sample. The PNIPAAm terpolymer was obtained by free radical polymerization of NIPAAm, MAA, and MaBP, initiated by AIBN. The polymerization solvent was dioxane. The reaction was carried out at 60 °C under argon for 24 h. A scheme of the polymerization reaction is shown in Figure 1. The polymer was precipitated directly from the reaction mixture in ice cold diethyl ether, purified by reprecipitation from methanol into ice cold diethyl ether, and freeze-dried from tertbutanol. In the case of the attached tetramethylrhodamine dye, a PNIPAAm sample was first activated with trifluoroacetyl-*N*-succinimidyl ester and then labeled with tetramethylrhodamine cadaverine. The activation was performed in dichloromethane at room temperature for 3 h in the presence of triethylamine. Purification was achieved by precipitation in diethylether twice.

Labeled PNIPAAm. Addition of the tetramethylrhodamine cadaverine to the activated polymer was achieved by stirring in ethanol at 50 °C for 20 h. In order to remove nonbound dye molecules, the polymer solution was subjected to dialysis in ethanol (MWCO of 3500 g/mol for the utilized tube) for 2 weeks.

PNIPAAm Gel. For the FCS studies, PNIPAAm gels were prepared on round glass microscope cover slides (Menzel-Glaser, Germany). As untreated surfaces of the cover slides are moderately hydrophobic, gel adhesion was promoted by first treating them with silane**1**. The latter was chemisorbed on the glass surface at room temperature from a toluene solution (20 mL of a 0.025 molar solution) using triethylamine (4 mL) as catalyst and acid scavenger. The solution with the glass substrates was left to stand overnight. Then, the samples were cleaned by successively rinsing with dichloromethane, methanol, toluene, and again dichloromethane. After each rinsing step, the sample was blown dry with nitrogen. PNIPAAm films of about 1 μm thickness were prepared by spin-coating from 10% w/w ethanol solutions onto the silanized microscope slides at 4000 rpm for 1 min. The samples were then dried over night at 55 °C and under vacuum conditions. Cross linking of the PNIPAAm films was performed by UV irradiation at $\lambda = 365$ nm for different times (from 10 to 240 min).

Photon Correlation Spectroscopy (PCS). The structure and dynamics of dilute and nondilute PNIPAAm/ethanol solutions were examined by PCS using an ALV-5000 digital correlator as described elsewhere.[15] The relaxation function $C(q,t) = \{[G(q,t) - 1]/f^*\}^{1/2}$ for the concentration fluctuations at a scattering wavevector q was computed from the experimental intensity autocorrelation function $G(q,t) = \langle I(q,t)I(q,0)\rangle/|\langle I(q)\rangle|^2$. $f^* < 1$ is an instrumental coherence factor and $q = (4\pi n/\lambda_0)\sin(\theta/2)$ is computed from the scattering angle θ, the refractive index n of the solution, and the wavelength λ_0 of the laser beam. For dilute solutions of monodisperse polymers, the exponential decay relaxation function

$$C(q,t) = \alpha \exp(-D_0 q^2 t) \tag{1}$$

yields the chain translational diffusion $D_0 = k_B T/(6\pi\eta_s R_h)$ and the net intensity $\alpha I(q)$ associated with the solute polymer; k_B is the Boltzmann constant, T the absolute temperature, R_h is the hydrodynamic radius, and η_s is the solvent shear viscosity. The absolute light scattering intensity $R_{vv} = \alpha I(q = 0)(n/n_t)^2 R_t/I_t$ with n_t, I_t, and $R_t = 2.7 \times 10^{-5}$ cm^{-1} being the refractive index ,intensity, and absolute Rayleigh ratio of the standard toluene yields the weight average molar mass $M_w = R_{vv}/(Kc)$ for sufficiently dilute solutions of PNIPAAm in ethanol. In order to obtain the optical constant $K = (2\pi n\, dn/dc)^2/(\lambda_0^4 N_A)$ where c is the polymer concentration (in grams per milliliter) and N_A is the Avogadro number, the refractive index increment $dn/dc = 0.152$ mL/g was measured at $\lambda = 633$ nm using a scanning Michelson interferometer. The molar mass M_w ($= R_{vv}/(Kc)$) amounts then to 305 ± 20 kg/mol using the experimental absolute intensity R_{vv} and the optical constant K. The polydispersity obtained by GPC amounts to $M_w/M_n = 2.2$. The Einstein diffusion coefficient D_0 in eq 1 yields to $R_h = 15 \pm 1$ nm for the PNIPAAm chain in dilute solutions in ethanol.

Fluorescence Correlation Spectroscopy (FCS). The FCS measurements were performed with a commercial FCS setup (Carl Zeiss, Jena, Germany) consisting of the module ConfoCor 2 and an inverted microscope model Axiovert 200. For all experiments, a 40x-C-Apochromat water immersion objective with a numerical aperture of 1.2 and a working distance of 0.29 mm was employed. Two fluorescent tracers were used: rhodamine 6G (Rh6G, Sigma-Aldrich) with $R_h = 0.8$ nm in ethanol and tetramethylrhodamine labeled PNIPAAm with $R_h = 19 \pm 1$ nm. Both tracers were excited with a He−Ne laser at $\lambda = 543$ nm, and the fluorescence emission was collected after filtering with a LP560 long pass filter. These arrangements result in a Gaussian confocal observation volume:

$$V_{obs}(x, y, z) = e^{-2((x^2+y^2)/r_0^2)}\, e^{-2(z^2/z_0^2)} \tag{2}$$

with $r_0 \sim 0.2$ μm and $z_0 \sim 0.8$ μm being the distances from the center of the beam focus. The fluorescence intensity fluctuations caused by the tracer diffusion through V_{obs} were detected with an avalanche photodiode enabling single-photon counting. Eight-well, polystyrene chambered cover-glass modules (Lab-Tek, Nalge Nunc International) were used as sample cells for the ethanol solutions of the PNIPAAm polymer. These cells had bottom slides with a high optical quality surface and a thickness of 0.17 mm. The tracer (Rh6G or rhodamine labeled PNIPAAm) concentrations were in the order of 10^{-8} M in these experiments. An Attofluor steel cell was used for the studies of the hydrogels. Before starting the FCS measurements, the quantity of 1 mL of ethanol was added in the cell, and the gel was allowed to swell until it reached an equilibrium state. The Rh6G tracer was then added to a final concentration of about 10^{-8} M. The FCS measurements were initiated 30 to 60 min later in order for the probe to reach the equilibrium concentration in the sample. Furthermore, multiple measurements made at different positions in the gel have shown very similar results. At each position, a series of 10 measurements with a total duration of 5 min were

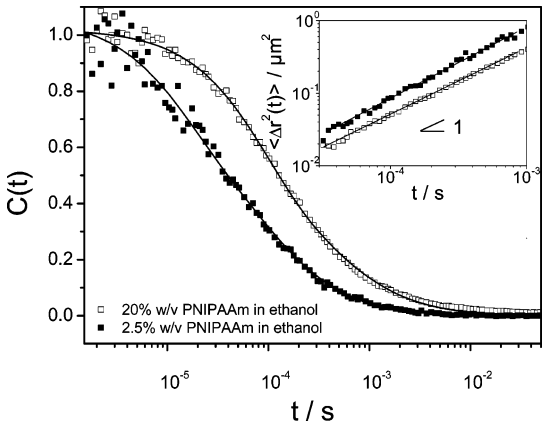

Figure 2. Normalized fluorescence intensity correlation function $C(t) = G(t) - 1$ (symbols) for Rh6G in two PNIPAAm /ethanol solutions in the semidilute regime along with the fit (solid lines) of eq 3. The diffusive (slope one) mean square displacement (eq 4) of the Rh6G is shown in the double log plot in the inset.

performed. From the measured fluctuations of the fluorescent intensity an experimental autocorrelation function $G(t)$ was obtained. For an ensemble of M different types of freely diffusing tracers, $G(t)$ has the following analytical form:[12]

$$G(t) = \frac{1 + \frac{T}{1-T}\mathrm{e}^{-t/\tau_T}}{N}\left(\sum_{i=1}^{M}\frac{1}{(1+t/\tau_i)\sqrt{1+t/(S^2\tau_i)}}\right) + 1 \quad (3)$$

where M is the number of fluorescent components, N is the average number of fluorescent molecules in the detection volume, T and τ_T are respectively the fractional population and the decay time (in the range of 0.5−10 μs) of the triplet state, $\tau_i = r_0^2/4D_i$ is the characteristic diffusion time of the ith fluorescent component with self-diffusion coefficient D_i and $S = r_0/z_0$ is the structural parameter of the instrumental setup. Precise calibration of the confocal observation volume was done using a reference dye with known diffusion coefficient, Rh6G in water.

III. Results and Discussion

A. Small Probe (Rh6G) Diffusion. Net experimental correlation functions $C(t) = G(t) - 1$ for the diffusion of Rh6G in two PNIPAAm/ethanol semidilute solutions near and well-above the overlap concentration c^* (∼0.4 w/v %) at 20 °C are shown in Figure 2. The experimental $C(t)$ are adequately represented by eq 3 with $M = 1$, and the diffusion time $\tau_1 \equiv \tau_D$ in the illuminated volume is expectedly an increasing function of the PNIPAAm concentration. Owing to the very low fluorophore concentration, FCS allows for the computation of the tracer mean square displacement $\langle \Delta r^2(t) \rangle$ in the observation volume V_{obs} with lateral r_0 and vertical z_0 dimensions from ref 12c.

$$G(t) = N^{-1}[1 + (2/3)\langle \Delta r^2(t)\rangle / r_0^2] - 1[1 + (2/3)\langle \Delta r^2(t)\rangle / z_0^2]^{-1/2} \quad (4)$$

The inset to Figure 2 displays the $\langle \Delta r^2(t) \rangle$ of the small dye as a function of time t. In order to avoid any photophysical effect (triplet decay in eq 2), the initial decay times are excluded in the plot of $\langle \Delta r^2(t) \rangle$ versus t. The slope 1 (in the inset of Figure 2), $\langle \Delta r^2(t) \rangle \sim t$ indicates a purely random Brownian diffusion with some deviations at the highest concentration. From the known value of the self-diffusion coefficient of Rh6G in ethanol, the experimental τ_1 (eq 3) is directly translated to the self-diffusion $D_s(c)$ of the Rh6G in PNIPAAm/ethanol solutions covering the concentration range 1×10^{-4} to 0.2 g/cm^3 at 20 °C.

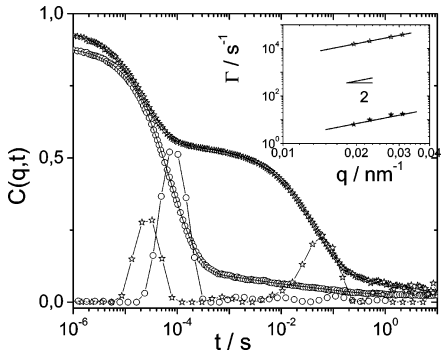

Figure 3. Relaxation function $C(q,t)$ for the concentration fluctuations in dilute ($c = 2.4 \times 10^{-3}$ g/cm^3 open circles) and semidilute ($c = 5.4 \times 10^{-2}$ g/cm^3) PNIPAAm/ethanol solutions at $q = 0.031$ nm^{-1}) along with the corresponding distribution of relaxation times. The two diffusive (slope 2) relaxation rates for the semidilute solution ($c = 5.4 \times 10^{-2}$ g/cm^3) are shown in the inset.

In the absence of specific interactions between probe and polymer segments, the decrease of $D_s(c)$ with the PNIPAAm concentration should reflect that of the viscosity $\eta_b(c)$ that captures the flow around the static (or mass) particle of diameter b. Since b is smaller than the size of the PNIPAAm chain, its motion should displace chain portions of size of the order of b.[16] Hence, $D_s(c) \sim \eta_b(c)^{-1}$ should be independent of the polymer molecular weight and display weaker c dependence than the macroscopic shear viscosity $\eta(c)$. This was pointed out some time ago in several investigations of particle sedimentation[9,17] and probe diffusion[8,18] in semidilute polymer solutions and gels. For the examined small probes, D_s was expressed as a function of the relevant length scales of the system, that is, the mesh size (ξ) of the polymer network and the particle size (b). In the proposed scaling behavior, that is, $D_s \sim \exp(-b/\xi)$, however, there was no independent information on the mesh size. Since this characteristic size of a transient polymer network at $c > c^*$ is approximately the correlation length $\xi(c)$ representing the average distance between two adjacent contacts, we have characterized the same PNIPAAm/ethanol solutions by PCS first.

Figure 3 displays the relaxation function $C(q,t)$ for the concentration fluctuations with wavevector q (= 0.031 nm^{-1}) in PNIPAAm/ethanol solutions at two concentrations in the dilute and semidilute regime. In the case of more than one decay, in order to analyze the relaxation function $C(q,t)$, we proceed through its inverse Laplace transformation,

$$C(q,t) = \int L(ln\ \tau)\ exp(-t/\tau)\ d ln\ \tau \quad (5)$$

where $L(\ln \tau)$ is the distribution of relaxation times. The relaxation rates $\Gamma = 1/\tau_{max}$ correspond to the peak positions of $L(\ln \tau)$ at τ_{max}, and the area under the peak defines the value of a (eq 1) and hence the intensity $aI(q)$ associated with the particular process. For dilute solutions, $C(q,t)$ displays a single process associated with PNIPAAm translational diffusion $D_0 = \Gamma/q^2$ which becomes the cooperative diffusion D_{coop} in the semidilute regime. In addition, a second slower process appears with also a diffusive (q^2 dependent) rate as shown in the inset of Figure 3. The D_{slow} ($= \Gamma_{slow}/q^2$) which appears to follow the concentration dependence of $\eta(c)^{-1}$ might relate to the self-diffusion of PNIPAAm (PCS active through polydispersity[19])

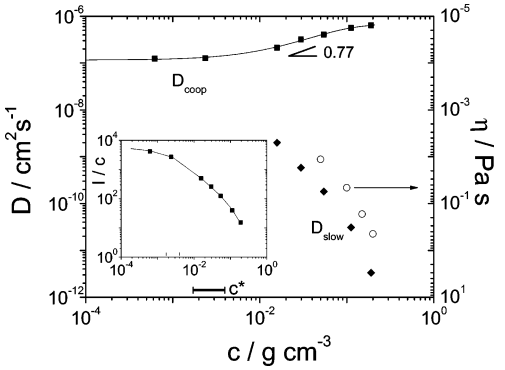

Figure 4. Cooperative D_{coop} and D_{slow} diffusion coefficients of PNIPAAm/ethanol solutions over a wide concentration range below and above the overlap concentration c^*. The solution viscosity is also shown as a function of concentration. The reduced I/c scattering intensity of the fast diffusion process is shown in the inset.

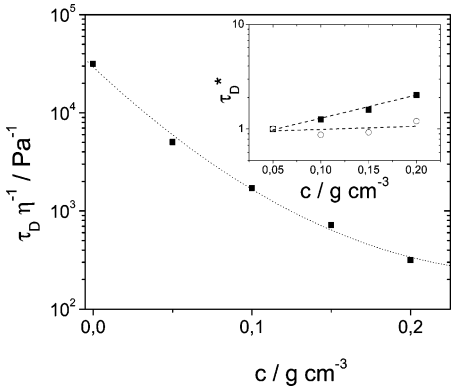

Figure 5. Diffusion time τ_D of Rh6G in PNIPAAm/ethanol solutions normalized to the solution viscosity as a function of PNIPAAm concentration. Inset: two proposed relations for the reduced diffusion time τ_D^* with the mesh size ξ are shown as a function of polymer concentration: $\tau_D(c)\exp(-b/\xi(c))$ (solid symbols) and $\tau_D(c)(\xi(c)/b)^{5/3}$ (open symbols).

or most likely to cluster diffusion[20] (see section III.B). The crossover to a semidilute solution at $c \sim c^*$ is marked by an increase of $D(c)$ and concurrent decrease of $I(c)$ with polymer solute concentration c because of the increase of the solution osmotic pressure. This behavior is clearly depicted in Figure 4 with $c^* \sim 3 \times 10^{-3}$ g/cm^3. In the semidilute regime, $D_{coop}(c) = k_BT/(6\pi\eta_s\xi)$ defines the mesh size $\xi(c)$ of the polymer network; $D_{coop}(c)$ display slightly weaker concentration dependence than the good solvent scaling $c^{0.77}$ prediction (solid line in Figure 4) over the examined semidilute range $1 < c/c^* < 70$. Since for a theta solvent the predicted scaling is even stronger ,the observed $D_{coop}(c)$ might be due to the PNIPPAm size polydispersity.

Returning now to $D_s(c)$ ($\sim \tau_D^{-1}$) of the small dye Rh6G, it becomes apparent from the plot of τ_D/η versus concentration in Figure 5 that the solution viscosity $\eta(c)$ increases much stronger with c than the dye self-diffusion time, $\tau_D(c)$. According to the proposed scaling,[16,17] $\tau_D^* \equiv \tau_D(c)\exp(-b/\xi(c))$ should be virtually independent of the polymer concentration. This is, however, not the case since the quantity τ_D^* increases by a factor of 2 in the examined concentration range as shown (solid symbols) in the inset to Figure 5. For the diffusion of small particles in an ensemble of Rouse chains with monomer concentration $c = l^{-3}$, the scaling relation, $\tau_D \propto b^3/l^2$, where l is a monomer size, has been proposed.[16] Transferring this physical picture of polymer melts to semidilute solutions with $c = \xi^{-3}$ in a good solvent, the diffusion time for the probe with

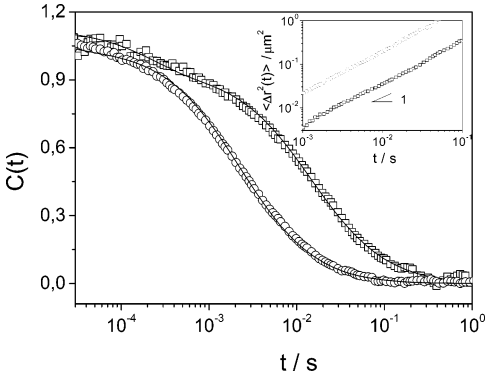

Figure 6. Normalized fluorescence intensity correlation function $C(t) = G(t) - 1$ for labeled PNIPAAm in two PNIPAAm /ethanol solutions with $c = 0.02$ g/mL (circles) and $c = 0.15$ g/mL in the semidilute regime. The diffusive (slope one) mean square displacement of the single PNIPAAm chain obtained from the slow decay of $G(t)$ is shown in the double log plot in the inset.

size b reads $\tau_D(c) \propto b(b/\xi(c))^{1/\nu}$ with $\nu \approx 3/5$ and is concentration dependent but polymer molecular weight independent. According to this scaling, the quantity $\tau_D^* \equiv \tau_D(c)\,(\xi(c)/b)^{5/3}$ should be insensitive to the variation of polymer concentration. In fact, this τ_D^* (open points in the inset to Figure 5) displays a much weaker concentration dependence as compared with the alternative exponential relation. This corroborates the notion that the observed slowing down of the small probe diffusion, roughly by a factor of 5, is mainly due to the reduction of the mesh size with polymer concentration better represented by the scaling relation. Conversely, this relation can be utilized to estimate an effective mesh size in chemically cross-linked and grafted gels (section III.C).

The finding that $\tau_D(c)$ does not follow the macroscopic viscosity $\eta(c)$ being a much stronger function of the polymer concentration was recognized in a recent FCS study of bulk amorphous polymers[13e] where $\tau_D(T)$ of a small probe at temperatures above the glass transition T_g mimics the $\tau_\alpha(T)$ of the primary α relaxation time of the polymer. In the same context, it was very recently reported[21] by XPCS measurements that nanoparticles can diffuse in polymer melts much faster than predicted by the Stokes−Einstein relation

B. Large Probe (PNIPAAm) Diffusion. The self-diffusion coefficient of polymers has received the most attention in the literature among various dynamic properties of the polymeric systems. It is usually measured by pulse-field gradient NMR,[22] optical grating techniques,[8,23] and, under some specific optical contrast conditions, by photon correlation spectroscopy.[11,19] FCS[12] has been applied to synthetic polymers only recently,[13] and hence, there is still limited information. In these techniques, the diffusion coefficient D_s of the labeled (tracer) polymer with molar mass M becomes independent of the matrix molecular weight M_m if M_m exceeds M[23b]. Since in the present study $M \approx M_m$, D is close to the self-diffusion and hence is expected to sense the global dynamics of the PNIPAAm nondilute solutions as reflected in the solution viscosity $\eta(c)$.

Figure 6 depicts normalized fluorescent intensity autocorrelation functions for the diffusion of the labeled PNIPAAm for two concentrations in the nondilute regime. These functions are clearly much slower than the corresponding decay functions for the small probe in Figure 2 at similar polymer matrix concentrations. The initial decay of $G(t)$ in Figure 6 (between 0.1 and 0.4 ms) might be due to the presence of a small amount of free dye (cf Figure 2). Excluding this initial decay, the tracer mean square displacement in the inset to Figure 6 conforms to a

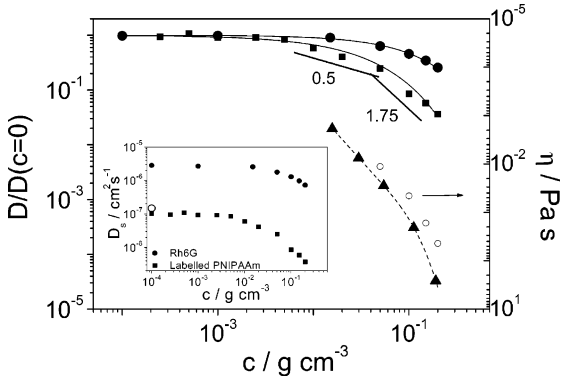

Figure 7. Normalized self-diffusion coefficient for the two indicated dyes in PNIPAAm/ethanol solutions over wide concentration range below and above the overlap concentration c^* ($\sim 3 \times 10^{-3}$ g/mL).The two solid lines represent a two parameter fit of the stretched exponential $\exp(-\beta c^x)$. For comparison, the solution viscosity (open circles) and the cluster diffusion coefficient (solid triangles) are also shown as a function of concentration. The dashed line through the latter is to guide the eye. Inset: the experimental self-diffusion coefficients of the two dyes (solid symbols) and translation diffusion coefficient (single open circle) of the PNIPPAM from the PCS experiment are shown as a function of concentration.

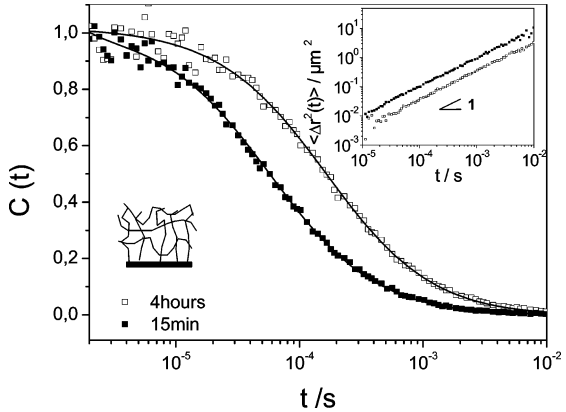

Figure 8. Normalized fluorescence intensity correlation function $C(t) = G(t) - 1$ for Rh6G in two graft (lower inset) cross-linked PNIPAAm films prepared under two different UV exposure time and subsequent swelling in ethanol. The diffusive (slope one) mean square displacement of the single R6Gh is shown in the double log plot in the inset.

random Brownian diffusive motion even at the highest concentration in agreement with the forced Rayleigh scattering experiments in polystyrene nondilute solutions[23b]. The inset to Figure 7 shows the diffusion coefficients D of the small and large probe along with the translational diffusion (open circle) of PNIPAAm measured by PCS; the latter is about 10% faster because of its slightly lower R_h compared with the labeled chain. The good agreement between FCS and PCS in dilute solutions is to be expected[13g] for correct experiments. The vastly different Einstein diffusion coefficient D_0 of the small and large probe in the dilute regime reflects the disparity of their sizes. For a clear presentation of the concentration dependence, Figure 7 displays the normalized diffusion coefficients relative to the corresponding (D_0) values at the lowest PNIPAAm concentration. The large probe diffusion clearly exhibits stronger concentration dependence than the small probe[8,16,23b] and resembles that of the solution viscosity shown in Figure 7 for comparison.

The concentration dependence of $D(c)$ for the large probe in a matrix with similar size should resemble the concentration dependence of the self-diffusion coefficient. Hence, the scaling predictions -0.5 and -1.75 respectively for unentangled and entangled semidilute solutions in a good solvent are drawn for comparison in Figure 7. The solution viscosity, shown for comparison in Figure 7, should exhibit stronger concentration dependence than the self-diffusion with corresponding scaling predictions 2 and 3.9 in the two semidilute regimes.[24] Experimentally, the specific viscosity, $\eta(c) - \eta_s \sim c^{3.4}$, in the highest concentration region is closer to the scaling exponent for entangled polymers in good solvents. The conformity to the scaling predictions up to the highest concentration suggests that the local friction does not play a significant role up to 20 vol %; that is, the solution is still semidilute in spite of the high T_g ($\sim$140 °C) of PNIPAAm.

The $D(c)$ data for the large probe can be also represented by smooth curves[13f,18] such as the empirical stretched exponential, $D(c)/D(c = 0) = \exp(-\beta c^x)$ proposed long ago.[10,25] The two adjustable parameters assume the values, $\beta = 11 \pm 3$ and $x = 0.71 \pm 0.08$. Apart from deviations, the physical meaning of these values relate to their association with material parameters and hence the dependence on the diffusant characteristics. Applying the stretched exponential equation to the small probe diffusion [section III.A], we find the two adjustable parameters now assume the values $\beta = 5.7 \pm 0.7$ and $x = 0.87 \pm 0.06$ representing well the experimental $D(c)$. The parameter β is proportional to the size of the diffusant, and the exponent x characterizes the particular system.[13g,17] For small diffusants, x was ascribed[17] to the concentration dependence of the mesh size $\xi(c) \sim c^{-0.77}$ (for good solvents). However, access to the experimental $\xi(c)$ and better performance of the scaling relation (inset to Figure 5) renders the association of the exponent x to known physical parameters of the nondilute polymer solutions ambiguous. In the same context, while the size ratio of the two diffusants is about 20, the ratio between the values of β is only 2. It appears therefore that the concentration dependence of the normalized D in Figure 7 cannot be attributed to the different size of the tracers according to the stretched exponential. Instead, it rather arises from the size dependent friction[16] of the system. A failure of a scaling with b/ξ was recently reported for spherical particle diffusion in suspensions of flexible polymers[6] and rods[13g].

The compilation of the different diffusion data in Figure 7 obtained from two complementary experimental techniques clearly disputes the assignment of the slow diffusion process in the PCS experiment (Figure 3) to the self-diffusion.[20] Instead, this process relates to the diffusion of a cluster of PNIPAAm chains closely following the macroscopic solution viscosity. This assignment is further supported by the observation of the slow process in the semidilute solutions $c > c^*$. Figure 7 clearly shows that the self-diffusion in semidilute homopolymers can be safely measured only by FCS and not PCS, but both techniques can be complementarily employed. In the present case, FCS measures both local dynamics associated with length scales $O(\xi)$ and global dynamics over the size of the used probe in the semidilute entangled regime well above c^*, whereas PCS can safely measure the mesh size $\xi(c)$ and the concentration dependence of $\eta(c)$ via the slow cluster mode. In the very dilute regime ($c \ll c^*$), both techniques measure the chain translational diffusion with FCS being applicable even at extremely dilute conditions.

C. Grafted Cross-Linked PNIPAAm. In semidilute solutions of homopolymers, $\xi(c) \approx c^{-m}$, where $m = 0.77$ (good solvent) or $m = 1$ (theta condition). When a semidilute solution is cross-linked, it is not safe[26] to assume that the average distance between the chemical cross links is still given by $\xi(c)$. This assumption becomes even poor if a grafted brush is cross-linked. In order to characterize structural changes upon cross linking,

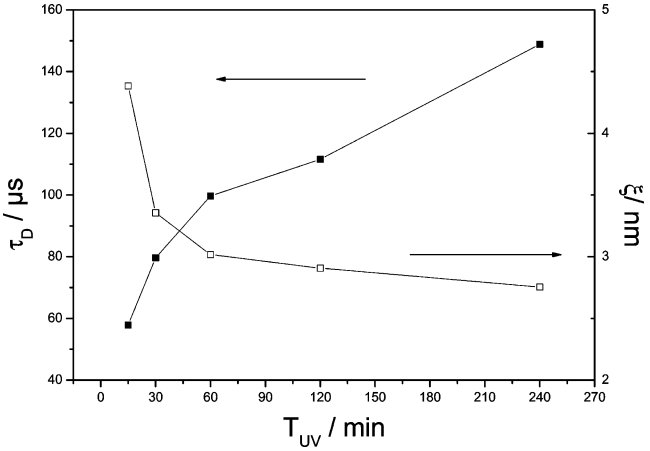

Figure 9. Diffusion time τ_D (solid points) of Rh6G in grafted cross-linked PNIPAAm/ethanol gels plotted as a function of the UV exposure time T_{UV} for the chemical cross linking of the grafted PNIPAAm. The computed average mesh size (open symbols) is a decreasing function of the cross-linking time.

nontrivial SANS measurements are needed. Instead, we could employ FCS to measure tracer diffusion and utilize τ_D to estimate an effective mesh size in grafted cross-linked PNIPAAm. In addition, we can estimate the swelling ratio κ of the gels prepared for a given UV exposure time T_{UV} through scanning of the probed volume from the glass substrate to the bulk solvent; the swelling ratio κ was defined relatively to the thickness of the dry gel. The thickness of the grafted gel was between 4 and 8 μm (± 1 μm) for the examined cross-linking densities.

Figure 8 shows normalized correlation functions for the diffusion of Rh6G in UV cross-linked grafted PNIPAAm gels (cartoon in the inset) swollen in ethanol displaying $\kappa = 10.9$ and $\kappa = 4.5$ respectively for $T_{UV} = 15$ min and 4 h. Over this range of T_{UV}, we found that $\kappa \sim T_{UV}^{-0.3}$. Apparently, the prolonged UV exposure time T_{UV} promotes the cross linking as evidenced from the reduced swelling ratio and the slowing down of the small probe diffusion. Interestingly enough, the short and long T_{UV} times do not affect, however, the purely diffusive random translation of the probe as indicated by the slope in the upper inset to Figure 8 like for the semidilute solutions of Figure 2. This is a pertinent finding given the, in general, inhomogeneous structure of gels.[26] This might be due to the fact that the time interval of the small dye in V_{obs} (eq 1) is short to experience the immobilized medium and attain long-time limiting diffusion[13g]. The diffusion time $\tau_D(T_{UV})$ obtained from the representation of $C(t)$ by eq 3 is plotted in Figure 9 for five PNIPAAm gels prepared with different exposure times T_{UV}. The characteristic average mesh size ξ of these gels can be estimated assuming the relation $\tau_D(c) \sim (\xi(c)/b)^{-5/3}$ used for the semidilute PNIPAAm/ethanol solutions (inset to Figure 5). With this assumption, the average mesh size plotted in Figure 9 decreases to 2.7 nm for a cross-linking time of about 4 h. Longer T_{UV} exposure times do not seem to lead to a significant increase of the cross-linking density.

On an empirical basis, the relation between the diffusion time and the swelling ratio both obtained from the same FCS experiment can be found useful to characterize cross-linked and grafted gels swollen in different solvents. The present PNIPAAm gels swollen in ethanol were found to conform to the relation $\tau_D \sim \kappa^{-1}$ over the examined T_{UV} range. Given the complexity of the gels, this relation should depend on their preparation as well as on the swelling conditions', for example, solvent quality, temperature since it reflects inhomogeneities in the gels. The swelling equilibrium concentration, c_{eq} can be estimated by a direct comparison of the experimental $\tau_D(c)$ in the gel and the transient network of the semidilute PNIPAAm solutions (section III.A). In the grafted cross-linked gel swollen in ethanol, c_{eq} increases from about 5% to about 20% for 15 min and 4 h duration of the UV irradiation, respectively. Since gels exhibit finite elasticity, the elastic modulus $G(c) \sim k_BT/\xi^3(c)$ can be estimated from $\tau_D(c)$. In fact, it was recently reported that there is a linear correlation between the diffusion of a small dye and the elastic modulus of cross-linked poly(vinyl alcohol) gels[13d].

IV. Concluding Remarks

We reported on a new application of FCS in the field of synthetic polymers. The translational motion of a molecular (Rh6G) and macromolecular (PNIPAAm) tracer in transient and permanent PNIPAAm networks in ethanol at different concentrations (up to $c \sim 20$ vol %) and cross-linking densities at ambient conditions were found to exhibit a Brownian diffusion supported by the absence of specific interactions with the polymer matrix. The normalized diffusion coefficient $D(c)/D(c = 0)$ for the two probes in the transient PNIPAAm/ethanol networks displays a different concentration dependence which cannot be described by the empirical stretched $\exp(-\beta c^x)$ when β is bound to the diffusant size. Alternatively, the assumption of a size-dependent friction allows for the association of the molecular probe diffusion to the mesh size of the transient network (Figure 5) which is concentration dependent but molecular weight independent. A proposed scaling relation can be used to characterize the chemically cross-linked swollen PNIPAAm networks grafted on solid surfaces. The strong concentration dependent macromolecular probe diffusion is in accord with the enhanced friction in semidilute entangled polymer solutions. Predicting a length dependent mobility can be useful for the utility of PNIPAAm networks as hydrogels for biosensor applications. The thermal motion of dispersed noninteracting probes depends on the structure and dynamics of the network host on microscopic length scales, but a theory that takes into account these network characteristics is missing so far.

Acknowledgment. We thank Dr. U. Jonas for fruitful discussions and Mrs. A. Larsen and Mr. A. Best for technical assistance. Financial support by Deutsche Forschungsgemeinschaft (DFG) through the Priority Program "Intelligente Hydrogele" (SPP 1259, KN 224/18-1) and IKYDA (119/2007) is gratefully acknowledged. M.G. thanks the European Community for financial support in the framework of a Marie Curie Host Fellowship for Early Stage Research Training.

References and Notes

(1) Tanaka, T. *Phys. Rev.* **1978**, *A17*, 763−766; *Phys. Rev. Lett.* **1978**, *40*, 820−823.

(2) Sershen, S.; West, J. *Adv. Drug Delivery Rev.* **2002**, *54*, 1225. Harmon, M. E.; Kuckling, D.; Frank, C. W. *Macromolecules* **2003**, *36*, 162.

(3) Beines, P. W.; Klosterkamp, I.; Menges, B.; Jonas, U.; Knoll, W. *Langmuir* **2007**, *23*, 2231.

(4) Zhang, J.; Pelton, R.; Deng, Y. *Langmuir* **1995**, *11*, 2301.

(5) Jones, D. M.; Smith, J. R.; Huck, W. T. S.; Alexander, C. *Adv. Mater.* **2002**, *14*, 1130.

(6) van der Gucht, J.; Besseling, N. A. M.; Knoben, W.; Bouteiller, L.; Cohen Stuart, M. A. *Phys. Rev. E* **2003**, *67*, 051106.

(7) Lewis, G.; Coughlan, D. C.; Lane, M. E.; Corrigan, O. I. *J. Microencapsul.* **2006**, *23*, 677.

(8) Cheng, Y.; Prud'homme, R. K.; Thomas, J. L. *Macromolecules* **2002**, *35*, 8111.

(9) Tong, P.; Ye, X.; Ackerson, B. J.; Fetters, L. J. *Phys. Rev. Lett.* **1997**, *12*, 2363.

(10) Phillies, G. D. J. *J. Phys. Chem.* **1989**, *93*, 5029.

(11) Lodge, T. P.; Rotstein, N. A.; Prager, S. *Adv. Chem. Phys*. **1990**, *79*, 1.

(12) Rigler, R.; Elson, E. L. *Fluorescence Correlation Spectroscopy;* Springer-Verlag: New York, 2001. Lumma, D.; Keller, S.; Vilgis, T.; Raedler, J. O. *Phys. Rev. Lett.* **2003**, *90*, 218301. Shusterman, R.; Alon, S.; Gavrinov, T.; Krichevsky, O. *Phys. Rev. Lett.* **2004**, *92*, 048303.

(13) (a) Sukhishvili, S. A.; Chen, Y.; Mueller, J. D.; Gratton, E.; Schweizer, K. S.; Granick, S. *Macromolecules* **2002**, *35*, 1776. (b) Zettl, H.; Haefner, W.; Boeker, A.; Schmalz, H.; Lanzendoerfer, M.; Mueller, A.; Krausch, G. *Macromolecules* **2004**, *37*, 1917. (c) Matejicek, P.; Podhajecka, K.; Humpolickova, J.; Uhlik, J.; Jelinek, K.; Limpouchova, Z.; Prochazka, K.; Spirkova, M. *Macromolecules* **2004**, *37*, 10141. (d) Michelman-Ribeiro, A.; Boukari, H.; Nossal, R.; Horkay, F. *Macromolecules* **2004**, *37*, 10212. (e) Best, A.; Pakula, T.; Fytas, G. *Macromolecules* **2005**, *38*, 4539. (f) Liu, R.; Gao, X.; Adams, J.; Oppermann, W. *Macromolecules* **2005**, *38*, 8845. (g) Kang, K.; Gapinski, J.; Lettinga, M. P.; Buitenhuis, J.; Meier, G.; Ratajczyk, M.; Dhont, J. K. G.; Patkowski, A. *J. Chem. Phys.* **2005**, *122*, 044905.

(14) Toomey, R.; Freidank, D.; Rühe, J. *Macromolecules* **2004**, *37*, 882; Adamczyk, M.; Chen, Y. Y.; Gebler, J. C.; Johnson, D. D.; Mattingly, P. G.; Moore, J. A.; Reddy, R. E.; Wu, J.; Yu, Z. *Steroids* **2000**, *65*, 295.

(15) Kroeger, A.; Belack, J.; Larsen, A.; Fytas, G.; Wegner, G. *Macromolecules* **2006**, *39*, 7098.

(16) Brochard Wyart, F.; de Gennes, P. G. *Eur. Phys. J. E* **2000**, *1*, 93.

(17) Langevin, D.; Rondelez, F. *Polymer* **1978**, *19*, 875.

(18) (a) De Smedt, S. C.; Lauwers, A.; Demester, J.; Engelborghs, Y.; De Mey, G.; Du, M. *Macromolecules* **1994**, *27*, 141. (b) Petit, J. M.; Zhu, X. X.; Macdonald, P. M. *Macromolecules* **1996**, *29*, 70. (c) Tokita, M.; Miyoshi, T.; Takegoshi, K.; Hikichi, K. *Phys. Rev. E* **1996**, *53*, 1823.

(19) Jian, T.; Anastasiadis, S. H.; Semenov, A. N.; Fytas, G.; Adachi, K.; Kotaka, T. *Macromolecules* **1994**, *27*, 4762.

(20) Yuan, G.; Wang, X.; Han, C. C.; Wu, C. *Macromolecules* **2006**, *39*, 6207.

(21) Tuteja, A.; Mackay, M. E.; Narayanan, S.; Asokan, S.; Wong, M. *Nano Lett*. **2007**, *7*, 1276.

(22) (a) von Meerwall, E.; Grigsby, J.; Tomich, D.; van Antwerp, R. J. *J. Polym. Sci. Polym. Phys. Ed*. **1982**, *20*, 1037. (b) Callaghan, P. T.; Pinder, P. N. *Macromolecules* **1984**, *17*, 431. (c) Fleischer, G.; Appel, M. *Macromolecules* **1995**, *28*, 7281.

(23) (a) Leger, L.; Hervet, H.; Rondelez, F. *Macromolecules* **1981**, *14*, 732. (b) Kim, H.; Chang, T.; Yohanan, J. M.; Wang, L.; Yu, H. *Macromolecules* **1986**, *19*, 2737. (c) Antonietti, M.; Coutardin, J.; Gruetter, R.; Sillescu, H. *Macromolecules* **1984**, *17*, 782.

(24) Doi, M.; Edwards, S. F. *The theory of Polymer Dynamics;* Clarendon Press: Oxford, U. K., 1986.

(25) Cukier, R. I. *Macromolecules* **1984**, *17*, 252. Altenberger, A. R.; Tirrell, M.; Dahler, J. S. *J. Chem. Phys.* **1986**, *84*, 5122. Phillies, G. D. *Macromolecules* **1987**, *20*, 558.

(26) Horkay, F.; Hecht, A. M.; Geissler, E. *Macromolecules* **1994**, *27*, 1795. Narita, T.; Knaebel, A.; Munch, J. P.; Candau, S. J. *Macromolecules* **2001**, *34*, 8224. Ikkai, F.; Shibayama, M. *J. Polym. Sci. Part B: Polym. Phys.* **2005**, *43*, 617.